Georgiev, V. P., Markov, S., Vila-Nadal, L., Busche, C., Cronin, L., and Asenov, A. (2013) Multi-scale computational framework for the evaluation of variability in the programing window of a flash cell with molecular storage. In: 2013 Proceedings of the European Solid-State Device Research Conference (ESSDERC), Bucharest, Romania, 16-20 Sep 2013, pp. 230-233.

There may be differences between this version and the published version. You are advised to consult the publisher's version if you wish to cite from it.

http://eprints.gla.ac.uk/98615/

Deposited on: 16 February 2016

Multi-scale computational framework for the evaluation of variability in the programing window of a flash cell with molecular storage

Vihar P. Georgiev[1], Stanislav Markov[3], Laia Vilà-Nadal[2], Cristoph Busche[2], Leroy Cronin[2] and Asen Asenov[1§]
[1]Device Modelling Group, School of Engineering, University of Glasgow, G12 8LT Glasgow, UK
[§] Gold Standard Simulations Ltd., G12 8LT Glasgow, UK
[2]WestCHEM, School of Chemistry, University of Glasgow, G12 8QQ Glasgow, UK
[3]Department of Chemistry, The University of Hong Kong, HK SAR, China
e-mail: vihar.georgiev@glasgow.ac.uk

Abstract—**We report a modeling study of a conceptual non-volatile memory cell based on inorganic molecular clusters as a storage media embedded in the gate dielectric of a MOSFET. For the purpose of this study we have developed a multi-scale simulation framework that enables the evaluation of the variability in the programming window of a flash-cell with sub-20nm gate length. Furthermore, we have studied the threshold voltage statistical variability due to the presence of random dopant fluctuations and polyoxometalate (POM) distribution in the cell. The simulation framework and the general conclusions of our work are transferrable to flash cells based on alternative molecules used for a storage media.**

I. Introduction

In recent years interest in electronic, magnetic and optical structures and devices based on inorganic, organic, hybrid and nano-materials has increased significantly. The idea of molecular electronics was first proposed in 1973 when Aviram and Ratner speculated about organic molecules as components of electronic circuits [1]. Since then, the emerging field of molecular electronics typically utilizes switchable organic molecules anchored between nano-electrodes, such as the rotaxanes-based arrays demonstrated in a molecular-based RAM [2]. From an engineering perspective, however, organic molecular electronics raises questions of high resistance and power, low performance and problematic fabrication, reproducibility and reliability.

Here we study an alternative class of compounds known as polyoxometalates (POMs) (see Fig. 1), which are metal-oxide inorganic molecules formed by early transition metal ions and oxo-ligands [3], [4]. They are assumed to be more compatible with existing CMOS processes than organic molecules by virtue of the chemistry of the oxo-ligands being closer to that of SiO_2. The interest in POMs for molecular electronics stems from the fact that POMs are highly redox active molecules; they can also be doped with electronically active heteroatoms; they can form semiconducting and metallic states essential for low power electronics devices [4].
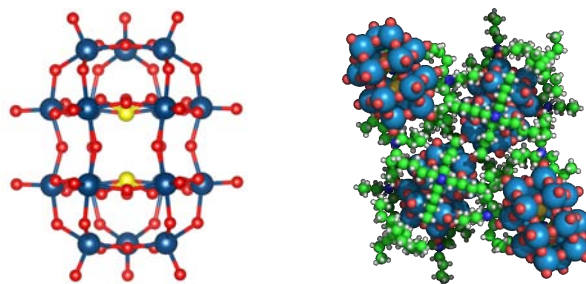

Fig. 1 Ball-and-stick view (left) on the non-classic Wells-Dawson [13], structure $[W_{18}O_{54}(SO_3)_2]^{4-}$ without (left) and with (right) counter cations at the vicinity of the molecule. W, O, and S are represented by blue, red and yellow spheres, $(CH_3H_7)_4N^+$ cation (tetrapropylammonium – TPA) – green.
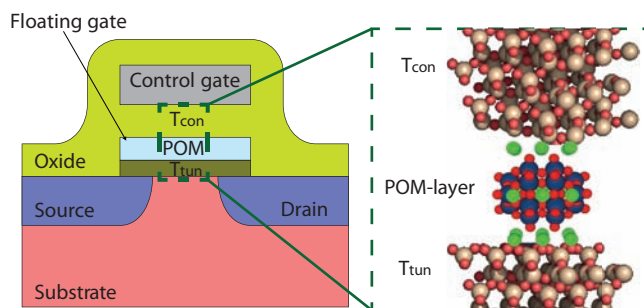

Fig. 2 Schematic representation of a single-transistor non-volatile memory cell, indicating the aimed substitution of the poly-Si floating gate (FG) with an array of polyoxometalate clusters (POM layer).

High electric conductivity and controllable conductivity through doping have been the cornerstones to the success of silicon nano-electronics, but unfortunately organic molecules have not yet demonstrated sufficiently attractive properties. POMs provide an unrivalled structural diversity of molecules, displaying a wide range of properties and nuclearities, and they are assembled under 'one-pot' reaction conditions allowing nano-scale objects to be self assembled from very small building blocks [4] based on MO_x, (where M is Mo, W,

V and x can be 4, 5, 6 or 7). Importantly, they can undergo multiple times reversible reduction/oxidation, which makes them attractive candidates for multi-bit storage in flash memory cells.

The use of redox-active molecules to form the storage media (FG) (see Fig. 2) could offer several very important advantages over the conventional polysilicon FG [5], [6]. For example, the charge storage is very localized, thus minimising cross-cell capacitive coupling (arising from charge redistribution on the sides of a poly-Si FG and being one of the most critical issues with flash memories). Although this benefit is present in floating gates realised by charge-trapping dielectric or by a metallic nano-cluster array, both technologies exhibit very large variability – charge-trap memories suffer variation in trap-density and trap-energy and the size and density of nano-clusters is difficult to control (this precludes their ultimate miniaturization). In fact, the concept of using molecules as storage centers has already been demonstrated for organic redox-active molecules [6], [12].

Here our intention is to study, by means of 3D simulations, the statistical variability of the threshold voltage of a non-volatile flash-memory cell, in which the charge-storing components constitute a layer of polyoxometalate molecular clusters (POMs) (see Fig. 2). The programmable charge embedded in the FG controls the threshold voltage, which is directly correlated with the conductivity of a transistor channel. The readout signal is the change in channel-current that corresponds to a change in the redox state of the molecules. Therefore, the principle of operation is like that of a charge-trapping memory, however, a conventional SiO_2 may be used as an insulator, due to the deep redox-levels of the POMs, and lower variability may be expected in terms of spatial and energetic distribution of the storage centers.

We emphasize that in the sub-20nm gate-length regime, the evaluation of variability is essential part of any feasibility study of a device. Variability arising from random dopant fluctuations (RDF) and POM fluctuations (POMF) is considered in the present study – the former known to be of largest impact in decananometer devices, the latter being anticipated due to POM-layer deposition or self-assembly.

II. FLASH CELL DESIGN

Here we summarize the key design parameters of our template flash memory cell, which are based on unpublished results. For the purpose of this study, an n-channel bulk flash memory cell with an 18 nm square gate has been designed (Fig. 2). It is based on a previously studied template of an 18 nm transistor [9] and is similar to the contemporary flash cells studied elsewhere [10]. The average acceptor doping in the channel of the transistor is just over 10^{18} cm^3. The high level of doping is necessary in order to maintain good electrostatic integrity at this ultra-short channel length.

Given that the gate area of the template flash cell is 18 x18 nm^2, we consider sheet densities N_S of POM clusters, approximately 3×10^{12} corresponding to nine metal clusters arranged in a 3x3 rectangular planar grid. From charge sheet approximation a 2 V programming window can be estimated for the first reduction state of all molecules in this
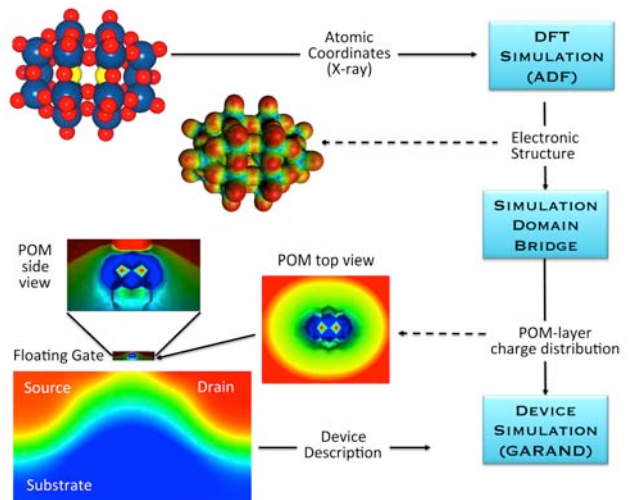

Fig. 3 Simplified block diagram of the simulation methodology, linking DFT and flash-cell modeling.
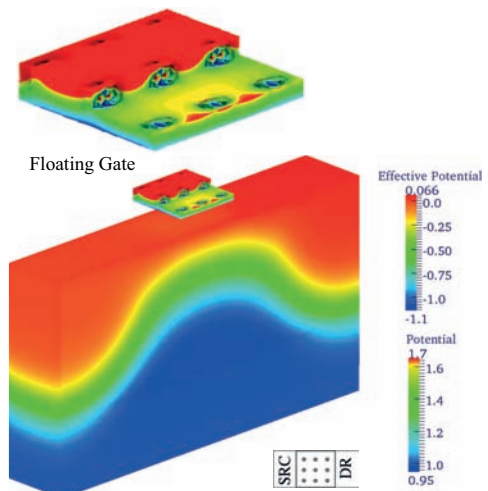

Fig. 4 Distribution of the potential and electrostatic potential in the simulated device with 3x3 regular grid of POMs; the oxide is cut away, exposing the local modulation of the potential, due to the charge stored in the nine POMs forming the floating gate.

arrangement, if the control oxide thickness T_{con} (see Fig. 2) is 15.6 nm. The tunneling oxide thickness T_{tun}, similarly to [6], consists of 3 nm high-quality SiO_2. The $[W_{18}O_{54}(SO_3)_2]^{4-}$ POM layer thickness is 3 nm, including the balancing cations, $(CH_3H_7)_4N^+$ (tetrapropyl-ammonium – TPA), forming an insulating barrier of permittivity very close to that of SiO_2 [14]. The POMs are oriented parallel relative to the SiO_2 surfaces. All simulations are performed at low drain bias ($V_{DS} = 50$ mV).

III. SIMULATION METHODOLOGY

In order to evaluate the performance of POMs for realization of a floating gate (FG) in flash-cell memories, we developed a simulation flow that links density functional theory (DFT) to the commercial three-dimensional (3D) numerical simulator GARAND [7]. The simplified diagram is presented in Fig. 3. Central to this flow is the custom-built *Simulation Domain Bridge*, connecting the two distinct
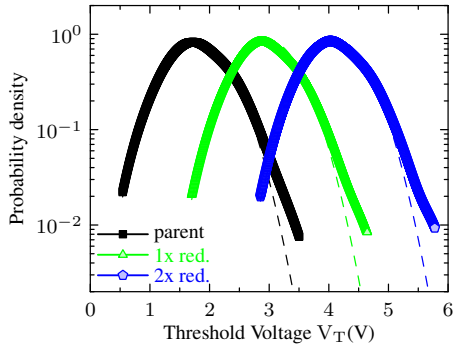
Fig. 5 Probability density function (PDF) of the V_T distribution for each bit 1000 bulk flash cells with *RDF only*. Dashed line is a Gaussian fit.
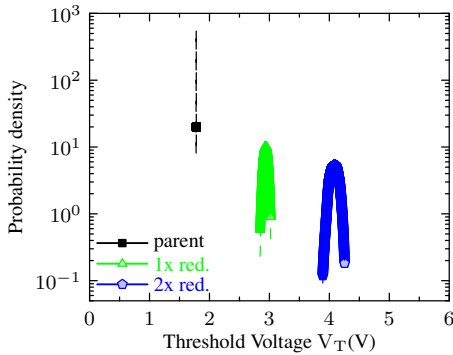

Fig. 6 Probability density function (PDF) of the V_T distribution for each bit 1000 bulk flash cells with *POMF only*. Dashed line is a Gaussian fit.
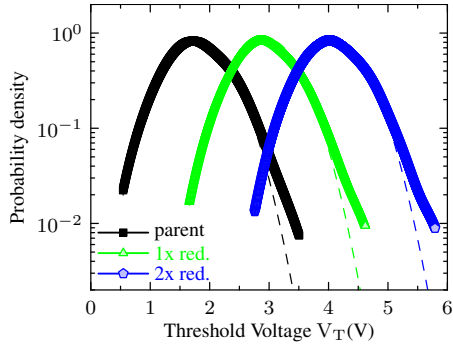

Fig. 7 Probability density function (PDF) of the V_T distribution for each bit 1000 bulk flash cells with combined variabilty – *RDF with POMF.*

simulation domains – DFT for the molecular part and mesoscopic device modeling section – GARAND for the device modeling part. The main motivation for using this plethora of computational techniques is the complexity of the problem. Accurate description of the POM clusters requires first principles calculations, which in this work are based on the DFT method. Moreover, the descriptions of the current flow through the devices demand the mesoscopic device approach provided by the GARAND software. The DFT calculations provide the atomic coordinates of the molecule together with molecular charge distribution for each redox state. This information is imported into the gate region of the transistors. In this way we are able to calculate performance of flash memory cells, using the GARAND software, where the

memory effect occurs due to configuration changes of the POM centers, which are induced by the gate electrodes.

The molecular simulations are based on the Amsterdam Density Functional (ADF) code [11]. A spin-unrestricted formalism is used with the gradient-corrected functionals of Becke and Perdew for the exchange and correlation energies, respectively (BP86). The valence electrons for all atoms are described with a Slater-type basis function of triple-ζ plus polarization quality. The inner electrons are kept frozen. Scalar relativistic corrections are included by means of the zero-order regular approximation (ZORA) formalism. The present computational settings, BP86/TZP, prove to be a satisfactory methodology for describing the electronic structure of polyoxometalates. All the structures discussed through this work are fully optimized taking into account the solvent effects by means of a continuous model. We have used the Conductor-like Screening Model (COSMO) as implemented in the ADF program package.

The spatial distribution of charge density, calculated from the DFT method for $[W_{18}O_{54}(SO_3)_2]^{4-}$ molecule at a given redox state, is used to construct fixed charge distribution representative of a POM layer with a controlled spatial and redox configuration of POMs. The metal cluster is negatively charged and, in order to keep the entire system neutral, in the experiment each POM is surrounded by positively charged molecules (cations – green structure in Fig. 1). Their presence is modeled within the device simulator as a set of fractional point charges distributed around the POMs, which is consistent with the COSMO approach used in the DFT calculation of the individual molecules. The total positive charge balances out the negative charge of the parent POMs, so that any reduction of the POMs leads to the presence of extra electron charges in the gate stack and redistribution of the negative charge density in the oxide.

Once the charge for the POM is obtained from the ADF program and it is transferred to the 3D numerical simulator GARAND a drift-diffusion transport formalism is applied. It includes quantum corrections by means of the density-gradient approach [8]. Results for flash cells with nine $[W_{18}O_{54}(SO_3)_2]^{4-}$ molecules in the floating gate are presented in the next section.

The programming/erasure of the cell is not studied here, although the anticipated mechanism is Fowler-Nordheim tunneling, as in charge-trapping memories. Presently there is no known approach to simulate the relevant transport problem through the gate stack and molecules in conjunction with the complex device electrostatics and substrate current.

IV. STATISTICAL VARIABILITY

In order to obtain realistic results for the programing window of bulk flash cell with molecules as a storage media, we introduced three sets of 1000 devices. Each set has two sources of statistical variability, such as random dopant fluctuations (RDF) and POMs fluctuations (POMF).We incorporate the charge density of the $[W_{18}O_{54}(SO_3)_2]^{4-}$ POM (shown in Fig. 1) as a charge storage center. Three, distinct V_T values related to the three easily accessible redox states of the molecular cluster can be obtained. They are presented in Table

Bits	Cont. Doping	RDF only 1000 devices		POMF only 1000 devices		POMF + RDF 1000 devices	
	μ (V)	μ (V)	σ (mV)	μ (V)	σ (mV)	μ (V)	σ (mV)
parent	1.778	1.821	448	1.778	0	1.804	458
1x red	2.948	2.976	443	2.936	32	2.948	454
2x red	4.107	4.122	437	4.081	66	4.082	455

TABLE I. COMPARISON OF THE STATISTICS OF THREE DIFFERENT V_T UNDER THE INFLUENCE OF RDF ONLY, POMF ONLY AND BOTH RDF+POMF WITH CONTINUOUS DOPING DEVICE.

I as follows: parent (neutral) POMs – no charge in the clusters; 1x red. – all POMs are ones reduced; 2x red. – all POMs are twice reduced.

Table I presents the statistics of an average value (μ) and the standard deviation (σ) of three different V_T values with only random dopants present (RDF only), with only POMs fluctuation present (POMF only) and with the combined RDF and POMF present. All results are compared to the nominal values of the flash cell with continuous doping.

It should be emphasized that for all three sets of 1000 devices composing the ensembles, the number of POMs is constant and it equals nine. In the case of the RDF only calculations, the charge storage centers are arranged in a regular grid of 3x3 POMs centered within the gate. Fig. 4 presents the electrostatic potential of a device with a regular grid of 3x3 POMs centered within the gate. In the POMF only calculations, the metal clusters are randomly displaced laterally with respect to the regular 3x3 grid used previously. Finally, in the third case, both of these variations are included, i.e., RDF and POMF.

Fig. 5, Fig. 6 and Fig. 7 present the same data from Table I but in a graphical form. Each figure shows the probability density function (PDF) for an ensemble of 1000 devices with RDF only, POMF only and RDF + POMF correspondingly. Based on our numerical calculations presented above we can obtain the following important conclusions.

Firstly, the curves presenting the PDF for all devices with RDF (Fig. 5 and Fig. 7) are significantly broader in comparison to the POMFs only case (Fig. 6). This reflects the values of the standard deviation presented in Table I where all flash cells with RDF have standard deviation close to 500 mV, while in the case of the POMF only calculations this value varies from 0 to 66 mV. Hence, it can be concluded that the RDF cells have significantly stronger impact on the σV_T in comparison to the POMF only calculations. Moreover, the two sources of variability show similar behavior and the main source of variability is indeed the RDF. However, in all calculations the results fit well with the Gaussian distribution (dashed line in Fig. 5 – Fig. 7) except for the tails of the curves. Such a discrepancy between analytical approximations and numerical calculations emphasizes the importance of numerical simulation in determining the devices' performance.

Secondly, for the continuous doping and RDF-only flash cells, the average value of V_T for each bit is almost identical. For the other two cases, POMF and RDF+POMF, we observe again almost identical values of the V_T but these results are shifted to lower values in comparison to the smooth and RDF calculations. This observation provides an important conclusion that the POMs determine the average value of V_T but the RDF is responsible for the standard deviation.

Lastly, the average value of V_T needed for the cell to change the oxidation state by one electron for each POM is 1.17 V in the case of continuous doping, 1.15 V in the case of RDF and POMF and 1.14 V in the RDF+POMF case, i.e., there appears to be a minor degradation of the average programming window. Moreover, probability density of the V_T distribution for each bit in Fig. 5 and Fig. 7 shows an overlap even before 3σ is reached. On the contrary, data presented in Fig. 6 (POMF only) reveals well-separated curves for each bit.

As a final note we should recall that flash variability is typically evaluated in conjunction with the ISPP (incremental step-pulse programming) algorithm [10]. This requires Kinetic Monte Carlo driven time-domain simulations, including the Fowler-Nordheim tunnelling current for programming, which will be the focus of our future efforts.

V. CONCLUSION

In this paper we presented the statistical variability for the programing window of the hybrid 18 nm BULK flash cell. Introducing of the $[W_{18}O_{54}(SO_3)_2]^{4-}$ POM in the floating gate (FG) of the cell shows a potential improvement of the device characteristics. Additionally, we established which source of variability is more influential for the statistics of V_T. Clearly, 'classical' sources of variability, such as the RDF cell, have more influence on the device performance in comparison to the spatial distribution and POMs' fluctuation in the FG.

REFERENCES

[1] A. Aviram and M. Ratner, "Molecular Rectifiers", Chem. Phys. Lett, vol. 29, pp. 277, 1974.

[2] J. E. Green et al., "A 160-kilobit molecular electronic memory patterned at 10^{11} bits per square centimetre", Nature, vol. 445, pp. 414, 2007.

[3] D.-L. Long et al., "Capture of periodate in a $\{W_{18}O_{54}\}$ cluster cage yielding a catalyticaly active polyoxometalate $[H_3W_{18}O_{56}(IO_6)]^{6-}$ embedded with high valent iodine", Angew. Chem. Int. Ed., vol. 47, pp. 4384, 2008.

[4] D.-L. Long et al, "Confined Electron Transfer Reactions within a Molecular Metal Oxide 'Trojan Horse' ", Angew. Chemie Int. Ed., vol. 44, pp. 3415, 2005.

[5] J. Lee et al. "Effects of floating-gate interference on NAND flash memory cell operation", IEEE Electron Device Letters, vol. 23, no. 5, pp. 264, 2002.

[6] J. Shaw et al., "Integration of self-assembled redox molecules in flash memories", IEEE Trans. Electron Devices, vol.58, no. 3, pp. 826, 2011.

[7] http://www.GoldStandardSimulations.com.

[8] A. Asenov et al., "Increase in the random dopant induced threshold fluctuations and lowering in sub-100 nm MOSFETs due to quantum effects: a 3-D density-gradient simulation study", IEEE Trans. Electron Devices, vol. 48, no. 4, pp. 722, 2001.

[9] S. Markov et al., "Drain Current Collapse in Nanoscaled Bulk MOSTETs Due to Random Dopant Compensation in the Source/Drain Extensions", IEEE Trans. Electron Devices, vol. 58, no. 8, pp. 2385, 2011.

[10] S. M. Amoroso et al."Three-dimensional simulation of charge-trap memory programming – Part II: Variability", IEEE Trans. Electron Devices, vol. 58, no. 7, pp. 1864, 2011.

[11] ADF 2008. 01, SCM, Theoretical Chemistry, Vrije Universiteit, Amsterdam, The Netherlands (http://www.scm.com).

[12] S. Paydavosi et al., "High-density charge storage on molecular thin films - candidate materials for high storage capacity memory cells", IEEE IEDM, 11-543, pp. 24-4-1, 2011.

[13] N. Fay et al., "Structural, Electrochemical, and Spectroscopic Characterization of a Redox Pair of Sulfite-Based Polyoxotungstates: α-$[W_{18}O_{54}(SO_3)_2]^{4-}$ and α-$[W_{18}O_{54}(SO_3)_2]^{5-}$", Inorg. Chem. , vol. 46, pp. 3502, 2007.

[14] N. Glezos, P. Argitis, D. Velessiotis, and C. Diakoumakos, "Tunneling transport in polyoxometalate based composite materials," Appl. Phys. Lett., Vol. 83, No. 3, pp.488–490, 2003.